Electrodeless Dielectrophoresis of Single- and Double-Stranded DNA

Chia-Fu Chou,*† Jonas O. Tegenfeldt,*† Olgica Bakajin,*‡ Shirley S. Chan,* Edward C. Cox,† Nicholas Darnton,* Thomas Duke,§ and Robert H. Austin*

Departments of *Physics and †Molecular Biology, Princeton University, Princeton, New Jersey USA; ‡Biosecurity Support Laboratory, Lawrence Livermore Laboratory, Livermore, California USA; and §Cavendish Laboratory, Cambridge University, Cambridge, United Kingdom

ABSTRACT Dielectrophoretic trapping of molecules is typically carried out using metal electrodes to provide high field gradients. In this paper we demonstrate dielectrophoretic trapping using insulating constrictions at far lower frequencies than are feasible with metallic trapping structures because of water electrolysis. We demonstrate that electrodeless dielectrophoresis (EDEP) can be used for concentration and patterning of both single-strand and double-strand DNA. A possible mechanism for DNA polarization in ionic solution is discussed based on the frequency, viscosity, and field dependence of the observed trapping force.

INTRODUCTION

Dielectrophoresis (DEP) is the translation of neutral matter caused by polarization effects in a nonuniform electric field (Pohl, 1978). Measuring and understanding the magnitude of the dielectrophoretic force exerted on important biopolymers such as DNA is a difficult fundamental problem that we address in this article.

An electrically polarizable object will be trapped in a region of a focused electric field, provided there is sufficient dielectric response to overcome thermal energy and the electrophoretic force. The standard way to make a DEP trap is to create an electric field gradient with an arrangement of planar metallic electrodes either directly connected to a voltage source (Washizu and Kurosawa, 1990; Muller et al., 1999) or free-floating (Washizu et al., 1994; Asbury and van den Engh, 1998) in the presence of an AC field. In this paper we use a constriction or channel in an insulating material instead of a metallic wire to squeeze the electric field in a conducting solution, such as ionic buffer, thereby creating a high field gradient with a local maximum. The advantages of the electrodeless DEP (EDEP) technology introduced here are: 1) no metal evaporation during the fabrication is needed; 2) the structure is mechanically robust and chemically inert; and 3) a very high electric field may be applied without gas evolution due to electrolysis at metal DEP electrodes. Fig. 1 outlines the differences between the metal electrode and the confined field technology of this paper. The simplicity of the device and the lack of metallic objects that cause electrochemical reactions involving gas evolution enable us to probe the response of DNA molecules well below 1 kHz, revealing a huge increase in the dielectric response at low frequencies (below 1 kHz), difficult to observe using metal electrodes as trapping structures.

The subject of this paper is not only the basic physics of dielectrophoresis, but also its applications to biotechnology. One of the great challenges in biotechnology is to move and concentrate molecules in a microfabricated environment. Notable applications of DEP include the separation of colloidal particles (Green and Morgan, 1999), DEP ratchets (Rousselet et al., 1994; Gorre-Talini et al., 1998), the separation of biological objects such as yeast cells (Pethig, 1996), viruses (Morgan et al., 1999), and cancer cells (Becker et al., 1995; Yang et al., 1999), and the trapping and manipulation of DNA molecules (Washizu and Kurosawa, 1990). EDEP can be used in all of the above-listed applications.

METHODS

The devices were fabricated on quartz wafers using reactive ion etching techniques, and sealed with a glass coverslip coated with an elastomer thin film to act as a sealing gasket. DNA dissolved in electrophoretic buffer was introduced into the sealed space and external gold electrodes attached to a high voltage source provided the external currents. It is important to understand a fundamental aspect of current flow in a basically *insulating* fluid such as water, namely that the current density **J** is proportional to the ion flux, since the ions carry the charge. Because it is the electric field that makes the ions move in the solution, in a backward way of saying it that we hope makes some sense, the electric field **E** is thus proportional to a hydrodynamic flow of charged ions. Thus, the electric fields are everywhere *parallel* to the surfaces of the constrictions in the insulating quartz, and the relative dielectric constants of the quartz and the water are irrelevant. Calculation of the electric fields is thus relatively easy, and no electric fields penetrate the insulating structures.

Fabrication

The device (see Fig. 1 *C*) was fabricated using UV lithography and reactive ion etching on 3-inch (76 mm) crystalline quartz wafers polished on both sides (Hoffman Materials, Carlisle, PA). The gaps in the quartz obstacles are 1 μm wide. Chips were diced out of the wafer and were 1 cm in length.

A 200-nm-thick aluminum film was thermally evaporated onto the quartz wafer and treated with hexamethyldisilazane (HMDS) in a Yield Engineering Systems LP-III Vacuum Oven to promote adhesion of the

Submitted November 5, 2001, and accepted for publication May 20, 2002.

Address reprint requests to Robert H. Austin, Dept. of Physics, Jadwin Hall, Princeton University, Princeton, NJ 08544. Tel.: 609-258-4353; Fax: 609-258-1115; E-mail: austin@princeton.edu.

0006-3495/02/10/2170/10 $2.00

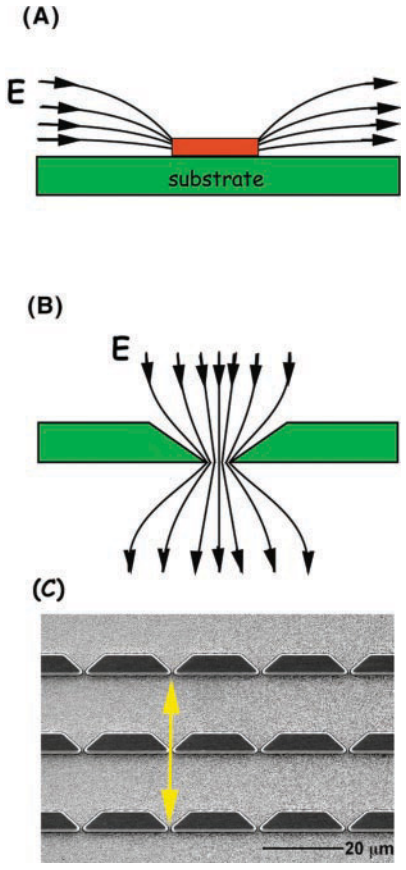

FIGURE 1 Schematic of a microfluidic DEP trap. (*A*) A metallic DEP trap made of microfabricated wire(s) on a substrate. The wire(s) may be either free-floating or connected to a voltage source. (*B*) An electrodeless DEP trap made of dielectric constrictions. The solid lines are electric field lines *E*. (*C*) A scanning electron micrograph of an electrodeless DEP device consisted of a constriction array etched in quartz. The constrictions are 1 μm wide and 1.25 μm deep. The whole chip measures 1 $\times$ 1 cm. The applied electric field direction *z* is shown by the double-headed arrow.

photoresist. Shipley S1813 (Microchem Corp., Newton, MA) photoresist was spun on the aluminum-coated quartz wafer at 4000 rpm in 60 s with a 3 s linear ramp. A pre-exposure bake at 115°C for 60 s was used. The wafers were exposed in a projection aligner (GCA 6300 DSW Projection Mask Aligner, 5x g-line Stepper). After development in MicroPosit CD26 (tetramethylammoniumhydroxide solution in water) (Shipley) for 60 s the aluminum is etched using a modified PK1250 ion etcher from PlasmaTherm. The PlasmaTherm PK1250 was also used to etch the quartz. Etch; times of 33 min resulted in an etch depth of 1.25 μm as determined by a Tencor AlphaStep 200 Surface Profilometer. The device was then sealed with a glass coverslip coated with silicone (polydimethylsiloxane) elastomer (RTV 615 A&B, General Electric, NY). Both the coated coverslip and the device were pretreated with oxygen plasma to make the surfaces hydrophilic and wettable when sealed. The top-sealed device was then wetted by capillary action with buffer solutions (pH 8.0, 0.5X Tris-borate-EDTA buffer (TBE), 0.1 M dithioDTT, and 0.1% POP-6). POP-6 is a linear polyacrylamide of proprietary formula provided to us by Applied Biosystems and serves to eliminate the transport of fluid in a sealed device due to bound charges on the quartz surfaces, known as electroendoosmosis (EEO). In the absence of POP-6, fluid is transported by ionic currents due to this surface effect, greatly complicating the forces acting on objects because of the added hydrodynamic transport.

Viscosity

Tests of the viscosity dependence of the EDEP force were carried out in 0.5X TBE buffer (pH 8.0 with 0.1% POP-6 and 0.1 M DTT). The viscosity was adjusted by adding sucrose to the buffer without changing the dielectric constant of the buffer (Chinachoti et al., 1988). The buffer viscosity of 3.7 cP was prepared by adding 46 g sucrose to 100 g buffer (31% w/w). The viscosity of 5.9 cP was prepared by adding 62.5 g sucrose to 100 g buffer (38% w/w). Viscosities were checked by viscometry at 20°C.

Electronics and imaging

A Kepco BOP 1000M amplifier with 1 kHz bandwidth provided the $\pm$1000 V driving voltage. The input to the Kepco BOP was provided by a HP 3325A signal generator which was connected via a GPIB interface to a MacIntosh computer running LabView (National Instruments) software. External gold electrodes driven by the Kepco BOP were immersed in liquid troughs that contacted the liquid, wetting the sealed chip. All voltages quoted in the text are the amplitude of the sinusoidal output of the BOP as measured by an HP 34401A digital multimeter. DNA was stained with TOTO-1 (1 dye molecule/5 bp) in 0.5X TBE buffer (pH 8.0 with 0.1% POP-6 and 0.1 M dithiothreitol (DTT). The images were gathered with a Nikon Microphot-SA microscope using an oil immersion objective lens (60$\times$, N.A.1.4), a cooled CCD camera (Hamamatsu C4880, NJ), and excitation at 488 nm by an Ar-Kr ion laser. Images of the DNA in the chip were taken by epifluorescence. The C4880 camera was run at $-$20°C.

DNA samples

We used five different double-stranded DNA with lengths of 368, 1137, 4361, and 39,936 bp, and a single-stranded DNA 137 nucleotides long. These were prepared as follows.

Double-stranded DNA

The 368-bp DNA was produced from an initial 54-base sequence. Both ends of the monomer duplex had complementary four-base overhangs. The monomer was kinased and ligated to create a multimer, then a ligation step was done at ~15°C to create a multimer ladder by varying the time of ligation from 6 to 24 h. Then a duplex with a 20-base primer sequence and a 24-base linker sequence was added to complete the ligation at both ends of the multimers. A quick spin column was used to wash away the monomer duplex, the primer-linker duplex, and the short ligated fragments ($<$200 bp). The multimers were then precipitated by cold ethanol, dried, and resuspended in TE buffer. A PCR step was performed on this ladder and analyzed by 1.8% agarose mini-gel. When two or three clean bands could be observed in an analyzing gel, a preparatory gel was run and the bands were cut to extract the fragments individually; then PCR was repeated in preparatory quantity to produce sufficient amounts (10–50 μg) of each fragment for experiments. The resulting product was cloned and sequenced. The GC content was 50% (the sequence is available from the authors). The 1137-bp DNA was prepared by PCR amplification of positions 2457–3594 of bacteriophage λ DNA. Before use, the PCR product was purified by standard methods from agarose gels.

The 4361-bp sample was prepared by digesting pBR322 DNA with *Bst*II and purifying the linearized DNA from an agarose gel. The 39,936-bp DNA is bacteriophage T7 DNA, and was purchased from Sigma Chemical and used without further purification.

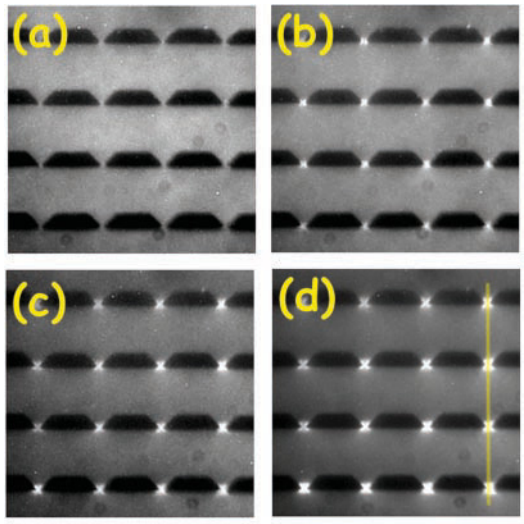

FIGURE 2 (*A–D*) Optical micrographs of DEP trapping of 368-bp dsDNA with driving voltage of 1 kV (corresponding to 5 V p-p across each unit cell) and applied frequencies of; 200, 400, 800, and 1000 Hz. The frame size is 80 × 80 μm. The images shown here were each averaged over three consecutive frames, starting with the first one taken 1 min after the AC electric field parameters were changed, and at 1-min intervals for each of the following images to allow equilibrium densities to be achieved. Equilibration typically occurred in a few seconds at each new field value. Each frame was exposed for 10 s and the light source was shut off when the camera shutter was closed to reduce photobleaching. The line shown in *D* shows the pixel swath used to analyze the density of the molecules in the trap.

1137 nucleotide ssDNA

Single-stranded λ DNA was prepared by amplifying the 1137-bp fragment (above). The primer homologous to the 2457 sequence was labeled at the 5′ terminus with biotin (BiotinTEG phosphoramidite, Glenn Research, Sterling, VA). The PCR reaction contained fluorescein-11-dUTP (Amersham Pharmacia, Piscataway, NJ) at a dTTP/dUTP-fluorescein ratio of 1:1. Single-stranded product was isolated by adsorbing the reaction mixture to Dynal-streptavidin beads (Dynabeads M-280, Dynal A.S., Oslo, Norway) and isolating single-stranded DNA from the beads by incubation at 0°C in 100 mM NaOH for a few minutes. Under these conditions the biotin-labeled strand remains attached to the Dynal beads, which are removed magnetically. The fluorescein-labeled single-stranded product in the supernatant was then concentrated and purified by ethanol precipitation and resuspension in buffer.

RESULTS

Basic results and dielectrophoretic force extraction

We first present a typical image of the basic data. Fig. 2 shows the image of trapped DNA density versus applied voltage for 368-bp-long fragments at an applied voltage of 1 kV across the cell as a function of frequency. At low frequencies there is basically no trapping; as the frequency is raised, the DNA molecules are attracted to the gap between the constrictions and the concentration of the DNA molecules in the gap increases. Clearly, the confinement of the electric field lines within the 1 μm gaps of the structures results in a powerful trapping of the molecules. The apparent force clearly rises with increasing frequency for this 368-bp-long sample. However, there are many parameters that must be explored to fully understand and exploit the ability of EDEP to trap and fractionate DNA molecules. Before we can proceed with explaining the way that EDEP can trap DNA molecules as a function of applied electric fields, field frequency, and size (length) of the molecules, it is important to have a quantitative way to analyze the trapping force felt by the molecules so that a physical model of the phenomena can be attempted.

In the absence of electrophoretic forces the *molecular* forces acting on single DNA molecules can be extracted from the images shown in Fig. 2. Because DNA at neutral pH is charged due to the phosphate groups, it also is transported by a DC electric field (electrophoresis); the following analysis is oversimplified and can give rise to misleading effective "forces," but does help to catalog the data. We will attempt to briefly discuss corrections later in this paper.

The trapping shown in Fig. 2 is due to the force a polarizable object feels in a field gradient. Charged polymers such as DNA at pH 7 are electrically neutral in the absence of an external electric field **E** because of the counterion cloud that surrounds the polymer. However, in the presence of an external field two things happen: 1) the movement of ions in the fluid shears away the counterions at the ζ potential surface, giving rise to a net charge density σ along the length of the polymer; and 2) the counterion charge distribution becomes polarized along the length of the molecules, giving rise to a dielectric moment **p**. Because the origin of the dipole moment is due to electrophoretic movement of counterions within the ζ potential surface, the induced dipole moment is a function of the applied electric field, the time over which the field is applied, and the size of the polymer. Typically, the induced dipole moment **p** is opposite to the direction of the applied field **E**, but this is not always the case. The Clausius-Mosotti (CM) ratio (Foster et al., 1992), which relates the sign of the dielectric force $\mathbf{F}_d$ to the gradient in the electric field energy density, can be either positive or negative, depending on the response of the material to the field (Pethig et al., 1992), although in our case the induced polarization is more complex in origin than the relatively simple displacement of charge within a molecule. Fig. 3 shows a cartoon of the way that the counterion cloud around a molecule of length L becomes polarized in an external field, leading to an induced dipole moment.

Let the distance z be the distance of a particle between the two external electrodes. The potential energy $U_p(z, \omega)$ of a polar but uncharged molecule in an applied field $\mathbf{E}(z, \omega)$ is:

$$U_p(z, \omega) = -\mathbf{p} \cdot \mathbf{E} = -\alpha(\omega)/2(E)^2 \qquad (1)$$

where α is the in-phase component of the complex polarizability of the molecule (Jackson, 1975) and includes the

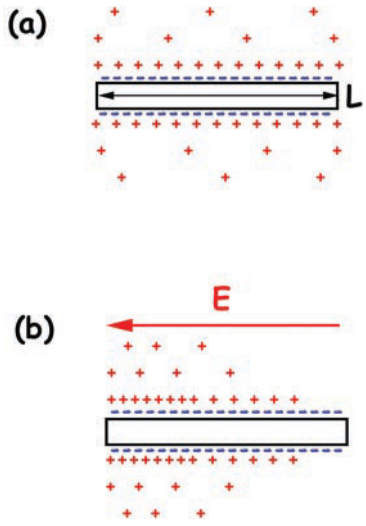

FIGURE 3 (*A*) Cartoon of the positive counterions surrounding a negatively charged DNA molecule of length *L*. (*B*) Distortion of the counterion cloud due to an externally applied electric field **E**.

CM term. DNA trapping only occurs when $U > kT$ and the CM factor is positive (positive EDEP).

The gradient in the potential energy $U(z, \omega)$ gives rise to a dielectrophoretic force $\mathbf{F}_d$:

$$\mathbf{F}_d = -\mathbf{grad}(U) = (\alpha/2)\mathbf{grad}(E^2) = \alpha|E|\frac{d\mathbf{E}}{dz} \quad (2)$$

where $|E|$ is the scalar magnitude of the field. This equation is the low-frequency limit of a generalized theory that can explain both DEP and the "laser tweezer" trapping observed when the wavelength of the radiation is smaller than the object (Ren et al., 1996). If the electric field has a local maximum, then a potential well is formed that traps the molecule because the field gradient changes sign around the maximum. At a finite temperature T the thermal energy kT broadens the distribution of molecules trapped in the potential well. In our system, a DNA molecule is driven by diffusional motion and an average drifting velocity **v** due to the external EDEP force $\mathbf{F}_d$ and the external electrophoretic force $\mathbf{F}_e$. The diffusion coefficient D and the average velocity **v** of a particle in the presence of an applied force **F** are linked through Einstein's relation: $\mathbf{v} = D\mathbf{F}/kT$, where D is the Brownian diffusion coefficient of a DNA molecule and kT the thermal energy. The flux of DNA molecules $J(z, t)$ at point z is governed by the modified Fick's equation:

$$\mathbf{J}(z, t) = \frac{D\mathrm{F}}{kT} \cdot n(z, t) - D\mathbf{grad}n(z, t). \quad (3)$$

where $n(z, t)$ is the local concentration of DNA molecules. At equilibrium, $\mathbf{J}(z, t) = 0$, the distribution of DNA molecules $n(z, t)$ obeys a Boltzmann distribution: $n(z, t) = n_o\exp[-U(z, t)/kT]$, where n_o is the density of DNA molecules at the minimum of the potential well.

In the limit of thermodynamic equilibrium the flux $\mathbf{J}(z, t)$ is zero and Eq. 3 allows us to analyze the local density of molecules $n(z, t)$ and extract the DEP force acting on them. The image analysis program NIH Image was used to extract a contour plot of the average density of the DNA across the constrictions (the scan region of the density plot is defined in Fig. 2), and computation of effective force from the density follows from Eq. 3:

$$F(z, t) = kT\frac{\mathbf{grad}[n(z)]}{n(z)} \quad (4)$$

where $\mathbf{grad}n(z)$ is the spatial gradient of the density distribution. Determination of the EDEP force is independent of n_o, provided a dilute DNA solution is used in which intermolecular interactions are negligible across the unit cell of the device. Note that the force is determined in absolute units, femtonewtons (fN), since we need only kT to get absolute units.

Many biological molecules are charged as well as polarizable (Takashima, 1989), and this complicates our analysis because there is also an electrophoretic force acting on charged molecules during dielectrophoresis. The net force is the sum of the two, and this complicates the analysis because the dielectrophoretic force always points toward the region of high field gradient and thus does not oscillate with the field direction change, while the electrophoretic force points along the direction of **E** and thus oscillates with the field direction change. If the electrophoretic force locally is greater than the dielectric force, the net translation $\Delta z \sim v_e\Delta t \sim \mu_e E(2\pi/\omega)$ can be large compared to the size of the dielectric trap. In that case, the assumption of thermodynamic equilibrium breaks down and the forces are not correctly determined; thus our analysis correctly describes the high-frequency response. At low frequencies the molecule is pulled out of the well by electrophoretic forces, and the apparent force is reduced due to a finite particle flux out of the trap.

Data and analysis

Fig. 4 shows the dielectrophoretic force exerted on the 368-bp molecule for a given field strength as a function of frequency and distance from the center of the trap. The force was extracted from the density distribution gradient using the pixel swatch shown in Fig. 2 *D*. Note how the force reaches its maximum not at the position of the strongest field (the center of the gap), but rather where the product of EdE/dz is largest. For the remainder of the analysis we will quote these peak values. It is clear from Fig. 4 that the dielectrophoretic force is a strong function of frequency. For the 368-bp sample, it rises with frequency to the 1 KHz limit of our amplifier. Fig. 4 shows how at 1 kV the maximum force in the trap rises monotonically with frequency. Although for 368-bp molecules we cannot measure the max-

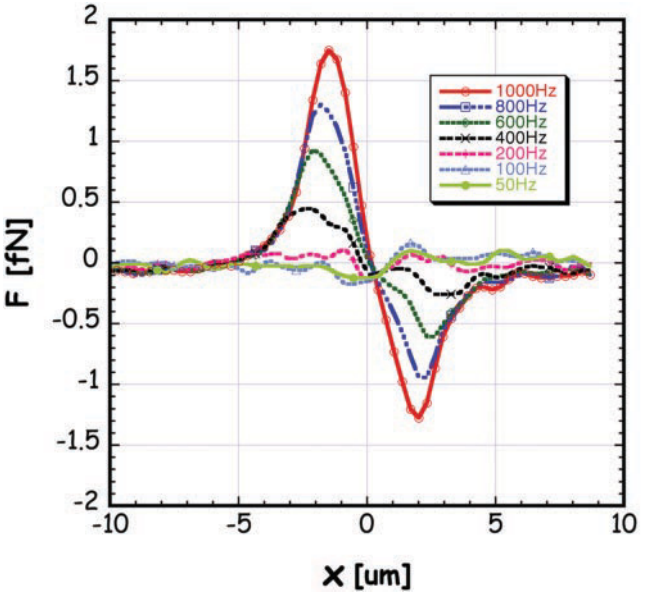

FIGURE 4 EDEP force response curve of 368-bp DNA with applied field 1000 V pp/cm (5 Vp-p per unit cell) as a function of frequency. Each curve is an average of all the unit cells in the microscope field of view.

imum frequency at which the EDEP response peaks with our current apparatus, longer lengths of DNA do show peaks in the trapping response with increasing frequency, as we shall show. We thus we believe the trapping frequency for this sample must also peak at higher values.

We discussed above the basic origin of this force, and in Eq. 2 showed that the trapping force should vary as the square of the electric field. For this to hold experimentally, it is necessary to ensure that the length of the molecule and the frequency of the applied field are such that the density of the trapped molecules has a spatial width great enough for us to easily extract the maximum force without the DNA concentrating into a band narrower than our optical resolution of ~0.5 μm. Fig. 5 illustrates this problem. At 1 kV and 200 Hz the 368-bp sample is barely trapped and data analysis is very difficult, while a 39.9-kb-long sample at 100 V and 100 Hz is trapped so tightly that analysis again is impossible. Fig. 6 shows that within our margin of error the force does scale as E^2 for the 1.1 kB sample using a 200 Hz frequency.

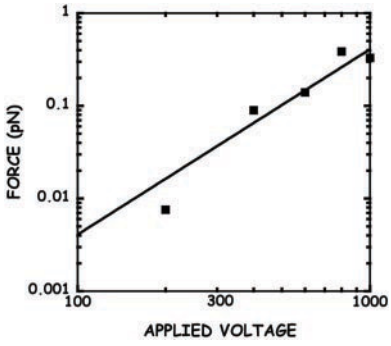

FIGURE 6 The measured peak force versus the applied voltage for the 368-bp DNA sample at 200 Hz plotted on a log-log scale. The solid line is a fit to these data assuming that the force varies as E^2. The only variable was the scaling parameter for the force magnitude.

We further show that the dielectrophoretic force greatly depends on the length of the DNA molecules. Fig. 7 shows the extracted forces for 368 bp and 1 kB samples as a function of frequency at 1 kV. Next, we show in Fig. 8 the peak forces as a function of frequency for 4361 bp and 39.9 kB DNA at 200 V. These measurements were done at a relatively low driving voltage of 200 V as opposed to the 1 kV values used in Fig. 7 because at the higher voltages the trapping force for long DNA molecules is so strong that we cannot accurately measure the width of the distribution (see above). Unlike the shorter fragment data, which show a monotonic rise in the trapping force with frequency, there is a hint of a maximum in response for the 4361-bp DNA and a very clear maximum in response for 39.9 kB DNA. Note that there is great dispersion in the force with length, hence by appropriate choice of parameters one can envision selectively trapping one range of DNA molecules while removing others.

We next examined the effect of solvent viscosity on the frequency dependence of the force. These experiments address the issue of the origin of the observed dielectric response of DNA: internal charge transport down the backbone of the DNA molecule, as would happen if DNA were a conductor, would be expected to result in a very fast response, while counterion flow within the Debye sheath of counterions near the DNA would be dominated by viscous drag. Fig. 9 shows the dependence of the EDEP force on our

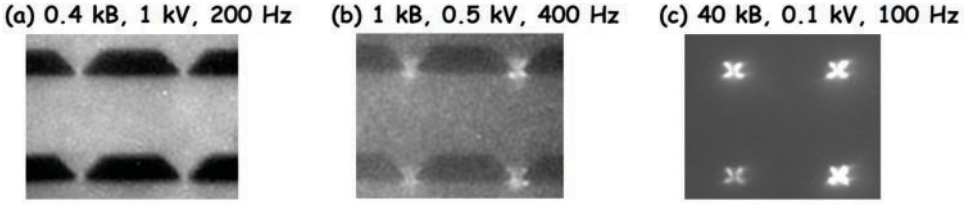

FIGURE 5 Images of the trapped DNA density as a function of length, voltage, and frequency.

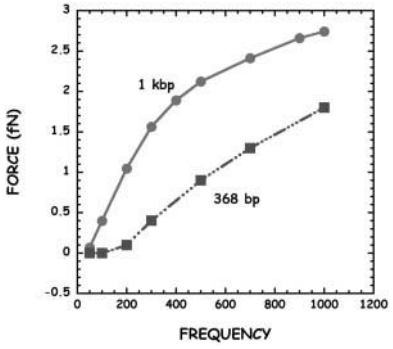

FIGURE 7 Force versus frequency for 1137-kB and 368-bp-long DNA molecules at an applied voltage of 1 kV.

longest DNA molecule over the three viscosities studied: 1 cP, 3.7 cP, and 5.9 cP. There is a clear shift of the frequency of maximum force response to lower frequencies with increasing viscosities.

Finally, we briefly explore the dependence of the EDEP force on single-stranded DNA (ssDNA). One would expect to find differences in the dielectrophoretic forces acting on two DNA molecules of identical molecular length, one ssDNA and the other dsDNA, because ssDNA has 1) half the linear charge density of dsDNA, 2) a different stacking conformation, and most importantly 3) a greatly different persistence length. The persistence length of ssDNA is believed to be much shorter than dsDNA. The persistence length of dsDNA is close to 50 nm, and somewhere between 1 to 6 nm for ssDNA (Smith et al., 1992, 1996; Tinland et al., 1997; Desruisseaux et al., 2001). Fig. 10 compares EDEP forces on dsDNA and an ssDNA molecule that have the same number of nucleotide units (basepairs for dsDNA, bases for ssDNA). Clearly, ssDNA experiences a substantially smaller force than dsDNA of the same number of nucleotide units.

ORIGIN OF THE LOW-FREQUENCY DIELECTROPHORETIC FORCE IN DNA

We now offer a simplified explanation for the length and low-frequency dependence of the EDEP experiments, a

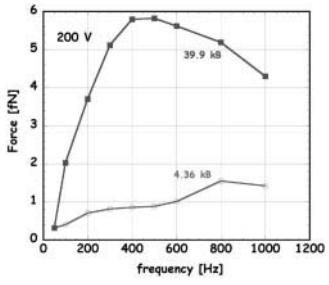

FIGURE 8 Force versus frequency for 4.36-kB and 39.9-kB-long DNA at an applied voltage of 200 V.

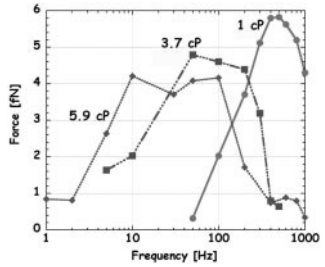

FIGURE 9 Force versus frequency and viscosity for a 39.9-kB DNA molecule.

complex subject we address briefly so that the reader can obtain an intuitive basis for the effects seen in the Methods section. We take as our fundamental starting point that the DNA backbone is an insulator consisting of fixed charges on the backbone with a surrounding layer of counterions. By noting the frequency dependence of the dielectrophoretic force on viscosity, we can further assume that when a DNA molecule is exposed to an externally imposed electric field **E** the surrounding counterion cloud becomes distorted by the diffusion of the counterions along the backbone (Porschke, 1985). This diffusion results in the formation of an electric dipole moment, but lagged in phase with the applied voltage. The resulting frequency dependence (dispersion) of the phase shift of the dipole moment on the polymer relative to the applied voltage from the external electrodes gives rise to a Debye-like relaxation process, which can be used to explain a large part of the frequency dependence of the dielectrophoretic force. In the words of the excellent paper by Foster et al. (1992), we confine ourselves to a dispersive object (the DNA polymer) in a non-dispersive solvent (water).

When charge moves along the length of a polymer, the polymer behaves like a capacitor C which is "charged" by the movement of the counterions along the backbone and from the surrounding solvent, resulting in an effective charge couple $\pm Q$ separated by some characteristic length d

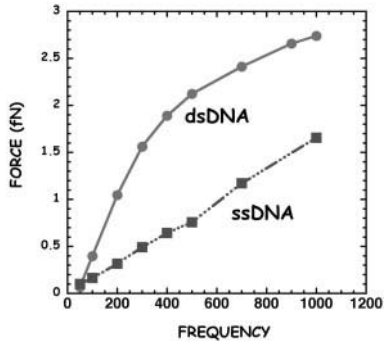

FIGURE 10 Force versus frequency for ssDNA and dsDNA of 1137 basepairs (dsDNA) and 1137 bases (ssDNA) at an applied voltage of 1000 V.

(see Fig. 3). The time for this charge couple to develop we call τ, rather like the charging time RC of a resistor in series with a capacitor, only in this case there is no resistor in series with the capacitor but rather a time-dependent charge build-up on the plate due to diffusion of the counterions, giving rise to the dispersion in the dielectric response.

The solution in the frequency domain for the frequency-dependent induced charge $Q(\omega)$ across the polymer is:

$$Q(\omega) = Q_o\left[\frac{1}{1 + (\omega\tau)^2} + i\,\frac{\omega\tau}{1 + (\omega\tau)^2}\right] \tag{5}$$

where Q_o is the DC induced charge. In the frequency domain the charge response of the molecule thus has an in-phase (real) response and an out-of-phase (imaginary) response due to the lag time of the polarization of the polymer as the ions diffuse along the backbone. The effective dipole moment $\mathbf{p} = Q(\omega)d$ thus has an in-phase (real) and out-of-phase (imaginary) response to the applied field, where d is some characteristic molecular distance that defines the separation of the charge on the molecule. Both Q_o and d are functions of the length of the polymer and the persistence length γ of the polymer. The in-phase component is the component parallel to the applied field and is the component that gives rise to the dielectrophoretic force. In terms of the notation used in Eq. 1, we have:

$$E\alpha(\omega) = \mathrm{Re}[Q(\omega)]d \tag{6}$$

Note that the polarizability as given by Eqs. 2, 5, and 6 goes to zero frequencies large compared to $1/\tau$ and has a finite value at zero frequency.

The relaxation time τ of the system can be viewed as the relaxation time RC of the capacitance of the polymer viewed as a charged object, and the resistance R of the counterion cloud that allows the charge separated on the ends of the molecule to flow together. Thus, the relaxation time τ of the response must be the diffusion time of the counterions across a distance x, which represents the mean size of the molecule. The fundamental relationship between τ and x is:

$$\langle x^2\rangle = 2D\tau \tag{7}$$

where D is the diffusion coefficient of the ions. The diffusion coefficient of the ions is related by Einstein's relationship to the ratio of the thermal energy k_BT to the frictional coefficient ζ of the ion:

$$D \sim \frac{\zeta}{k_BT};\quad \zeta \sim 6\pi\eta a \tag{8}$$

where η is the viscosity of the medium and a is some mean hydrodynamic radius. Monovalent ions such as Na^+ have diffusion coefficients on the order of 10^{-5} cm^2/s at room temperature in water of viscosity 1 cP (American Institute of Physics Handbook, 3rd Ed. 1972. American Institute of Physics, College Park, MD). In addition to the diffusion coefficient of the counterions, to estimate τ we have to have some idea of the size of the polymer that separates the charge. We should point out here that we consider only the diffusion of the counterions, not the diffusion of the center of mass of the polymer. The ability of the counterions to diffuse freely through the polymer is due to the free-draining nature of the hydrodynamics of a polymer undergoing electrophoresis (Volkmuth et al., 1994).

We need to point out here that the above analysis is surely oversimplified. We assumed that the dipole moment relaxes due to pure diffusive motion of the counterions, but of course the electric field generated by the dipole moment should enhance this relaxation rate. However, electric fields in an ionic medium are shielded by the counterions, and this greatly reduces the actual field due to the dipole across the molecule. An excellent review paper by Hoagland et al. (1999) gives a clear description of the physics of counterion shielding. The basic length scale for shielding by counter ions is the Debye length λ_D:

$$\lambda_D = \left[\frac{\epsilon k_BT}{4\pi k e^2 n_b}\right]^{1/2} \tag{9}$$

where ϵ is the dielectric constant of the fluid, e is the electron charge, k is Coulomb's law constant (9×10^9 Nt-m^2/C^2), and n_b is the number of ions/volume in the bulk solvent. For a 0.1 M salt concentration, λ_D is ~3 nm, so the screening distance is very short relative to the length of our molecules, and perhaps the field enhanced diffusion is not important.

Given, then, that the purely diffusive relaxation may overestimate relaxation times, we continue with it because it appears to give basically order of magnitude correct relaxation rates. We can consider easily two extreme cases: 1) long polymers, whose persistence length γ is much less than the extended length L of the polymer; and 2) short polymers, whose length L is much less than the persistence length γ.

In the case of a very long polymer, the diffusion distance x can be approximated by the mean separation between the two ends of the polymer $R = (2L\gamma)^{1/2}$ of the polymer. In the case of a short polymer, we can use $x \sim L$ because the polymer is simply extended roughly to its full length. Thus, we have for long polymers the relaxation time τ_{long}:

$$\tau_{long} = \frac{L\gamma}{D} \tag{10}$$

while for short polymers τ_{short}:

$$\tau_{short} = \frac{L^2}{2D} \tag{11}$$

These two expressions can be roughly used to predict the relaxation times, but should be taken with a grain of salt. For example, consider the T7 dsDNA data shown in Fig. 9,

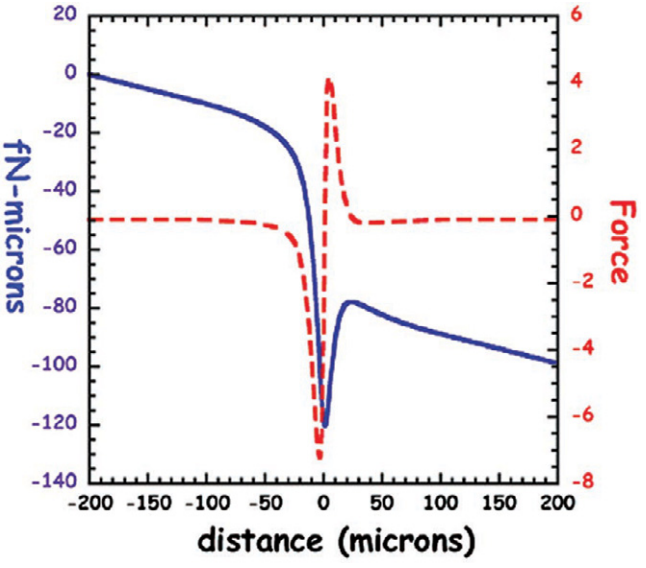

FIGURE 11 The measured relaxation time of 39.9 kB (T7 phage) DNA versus viscosity (*solid line*) versus the predicted relaxation time (*dashed* line).

which shows the EDEP force as a function of frequency and viscosity. Measurements at the two higher viscosities (3.7 and 5.9 cp) clearly show that the dielectrophoretic force decreases at high frequencies. This occurs at ~1 kHz for 1 cP, 300 Hz for 3.7 cP, and 150 Hz for 5.9 cP. Because T7 at 39.9 kB is definitely in the $L \gg \gamma$ case for long polymers, we can use Eq. 10 to estimate the relaxation time of these polymers. Fig. 11 shows the satisfactory agreement between the observed relaxation times and the ones predicted for a long polymer, considering the simplicity of the model used. Short polymers can be expected to have faster relaxation times. In the case of our 368-bp fragment, Eq. 11 predicts a relaxation time in water of $\sim 10^{-5}$ s, substantially beyond the present 1 kHz bandwidth of our high-voltage power supply.

Rough calculation of the force **F** felt by the polymer is more difficult, as we have mentioned. From Eq. 2 we know that the dielectric force is proportional to the product of the polarizability of the molecule α times $|E|\, d\mathbf{E}/dz$. The polarizability α is equal to Cx^2, where C is the effective capacitance of the molecule and x^2 is the mean-squared separation of the two charged ends of the molecule. In the rough approximation that the capacitance C is equal to $\epsilon\epsilon_o A/x$, where A is the area of the charged ends of the molecule, we once again find that the force also depends on the statistical mechanics of the polymer. If 1) $L \gg \gamma$, we get that $\alpha_{long} = \epsilon\epsilon_o[(2L\gamma)]^{3/2}$, while if 2) $L \ll \gamma$, we find that $\alpha_{short} = \epsilon\epsilon_o A_o L$, where A_o is an area that characterizes the end area of rigid length of the molecule. These numbers are rather poorly defined. The backward way to do this is simply to calculate from the measured force at a given **E** and $d\mathbf{E}/dz$ the polarizability α. As we have shown, α is a strong function of length and conformation of the molecule, so there is no single intensive parameter that characterizes DNA.

There is still a problem with this analysis. Equations 2 and 5 together imply that the EDEP force is effectively zero at high frequencies (which is not true because of other processes that come into play (Takashima, 1963; Oosawa, 1970)), rises at a frequency given by $1/\tau$, and then remains constant down to DC. In fact, all our data show the apparent force falling to zero at DC frequencies. The problem is that we have ignored the electrophoretic force. The total force acting on a polyelectrolyte in an external electric field is the sum of the electrophoretic force $\mathbf{F}_e$ due to the net effective linear charge density β of the polymer, and the dielectrophoretic force $\mathbf{F}_d$ due to the induced dipole moment **p** discussed above. The electrophoretic force $\mathbf{F}_e$ on a polyelectrolyte in the presence of a electric field is proportional to the local applied electrical field **E** and gives rise to a constant velocity $\mathbf{v}_e$:

$$\mathbf{v}_e = \mu_e \mathbf{E}; \quad \mathbf{F}_e = \zeta \mathbf{v}_e = \zeta \mu_e \mathbf{E} \tag{12}$$

where μ_e is the electrophoretic mobility of the polymer, $\mathbf{v}_e$ is the electrophoretic velocity, and ζ is the drag coefficient between the electrophoretic velocity and the force. The origin of the electrophoretic force $\mathbf{F}_e$ in polyelectrolytes has been intensively studied (Grossman and Colburn, 1997) and is characterized by the surprising fact that the electrophoretic mobility of a polyelectrolyte is basically independent of the length of the polymer in free solution, hence we can treat μ_e as a constant independent of length. We then have a final expression for the total force acting on a charged, polarizable polyelectrolyte:

$$\mathbf{F}_{tot} = \zeta \mu_e \mathbf{E} + \alpha |E| \frac{d\mathbf{E}}{dz} \tag{13}$$

An interesting aspect of the dielectric force is that it is a nonlinear force as a function of **E**, and hence at sufficiently high field strengths and sufficiently low ratios of μ_e/α a gradient can trap a molecule even in a static DC field, because the dielectrophoretic force will ultimately be greater than the linear electrophoretic force. By combining the electrophoretic and the dielectrophoretic response, we show in Fig. 12 the forces and potential surfaces that charged, polarizable objects experience going through a gap similar to one of our devices. The parameters for the polarizability α and the electrophoretic mobility μ_e were chosen here to roughly correspond to our longest molecules studied, the 40-kB dsDNA. Note that the nonlinear dielectrophoretic component of the trapping force gives rise to a short-range trapping potential. If the field direction is switched, the electrophoretic potential surface will slope in the opposite way while the dielectrophoretic potential is invariant, so that only the dielectrophoretic component of the force serves as a trap.

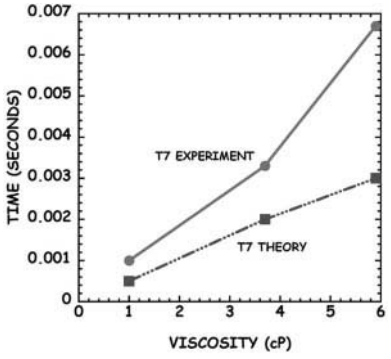

FIGURE 12 The total force, electrophoretic and dielectrophoretic, experienced by a particle passing through the gradient trap shown in Fig. 1 is presented as the dashed red line. The potential $U(z)$ surface that the particle moves along is shown by the solid blue line.

Because the free flow electrophoretic mobility μ_e is basically independent of length of the DNA molecule, the effect of electrophoresis of the molecule is an *apparent* decrease in the force at low frequencies if the electrophoretic force is greater than the dielectrophoretic force, which appears to be the case for DNA. In fact, the entire model we used to analyze the dielectrophoretic force acting on the molecules basically breaks down at low frequencies, as one of the referees of this paper has pointed out, because we do not have an equilibrium condition. At present, we have no way of disentangling the true dielectrophoretic force at low frequencies from the electrophoretic force.

CONCLUSIONS

We have used electrodeless EDEP to trap and concentrate single- and double-stranded DNA. The analytical simplicity of the field pattern in a electrodeless trap has allowed us to characterize the length and frequency-dependence of the EDEP force. We showed the strong dielectrophoretic response of the DNA in the audio frequency range. We also demonstrated that for the given trapping voltage applied, the dielectrophoretic force dramatically increases with the increase of the length of the DNA molecule. There is actually a great dispersion in the force with length, hence by appropriate choice of parameters one can envision selectively trapping one range of DNA molecules while removing others. By measuring dielectrophoretic force under different solvent viscosity conditions, we were able to determine that movements of counterions in the Debye layer are responsible for the dielectrophoretic response of the DNA for two reasons: 1) a strong dependence of relaxation times on solvent viscosity indicates that the charge redistribution occurs via movement through the solvent; and 2) the expected relaxation times due to diffusion of ions across the radius of gyration of the polymer are in rough agreement with the observed relaxation times.

The dielectrophoretic trapping of the DNA in electrodeless traps has a great potential for use in biotechnology. The EDEP force may be adjusted accordingly by varying the shape and cross-section of the constriction. Position of the constriction also can be controlled at will. Because EDEP trapping occurs in high field gradient regions, EDEP allows easy patterning of DNA by appropriate geometrical obstacle design. Other potential applications of the EDEP method are selective trapping of specific ranges of DNA; concentration of DNA molecules to very tight bands before launch into a fractionating media; PCR cleanup; concentration of DNA in gene array chips to enhance sensitivity of the detection limit by increasing local S/N, or acceleration of gene hybridization rates by concentration of single-stranded DNA; and in general for any reaction for which the rate scales with concentration or any power of the concentration greater than 1.

We are grateful to Professors Paul Chaikin, Nai-Phuan Ong, and Jacques Prost for helpful discussions, and Chang Guo Liu for assistance with the Ansys simulation program. Microfabrication of the device was done at the Cornell Nanofabrication Facility.

This work was supported by National Institutes of Health Grants HG01506 and GM55453, the Royal Society, and New Jersey Science and Technology Council Grant E08580.

REFERENCES

Asbury, C. L., and G. van den Engh. 1998. Trapping of DNA in nonuniform oscillating electric fields. *Biophys. J.* 74:1024–1030.

Becker, F. F., X. B. Wang, Y. Huang, R. Pethig, J. Vykoukal, and P. Gascoyne. 1995. Separation of human breast-cancer cells from blood by differential dielectric affinity. *Proc. Natl. Acad. Sci. U.S.A.* 92:860–864.

Chinachoti, P., M. P. Steinberg, and D. A. Payne. 1988. Measurement of dielectric constant to quantitate solute water in the sucrose-starch-water system. *J. Food Sci.* 53:580–583.

Desruisseaux, C., D. Long, G. Drouin, and G. W. Slater. 2001. Electrophoresis of composite molecular objects. 1. Relation between friction, charge, and ionic strength in free solution. *Macromolecules.* 34:44–52.

Foster, K. R., F. A. Sauerm, and H. Schwan. 1992. Electrorotation and levitation of cells and colloidal particles. *Biophys. J.* 63:180–190.

Gorre-Talini, L., J. P. Spatz, and P. Silberzan. 1998. Dielectrophoretic ratchets. *Chaos.* 8:650–656.

Green, N. G., and H. Morgan. 1999. Dielectrophoresis of submicrometer latex spheres. *J. Phys. Chem. B.* 103:41–50.

Grossman, P. D., and J. C. Coburn (editors). 1997. Capillary Electrophoresis: Theory and Practice. Academic Press, New York.

Hoagland, D. A., E. Arvanitidou, and C. Welch. 1999. Capillary electrophoresis measurements of the free solution mobility for several model polyelectrolyte systems. *Macromolecules.* 32:6180–6190.

Jackson, J. D. 1975. Classical Electrodynamics, 2nd Ed. John Wiley and Sons, New York.

Morgan, H., M. P. Hughes, and N. G. Green. 1999. Separation of submicron bioparticles by dielectrophoresis. *Biophys. J.* 77:516–525.

Muller, T., G. Gradl, S. Howitz, S. Shirley, T. Schnelle, and G. Fuhr. 1999. A 3-D microelectrode system for handling and caging single cells and particles. *Biosens. Bioelectron.* 14:247–256.

Oosawa, F. 1970. Counterion fluctuation and dielectric dispersion in linear polyelectrolytes. *Biopolymers.* 9:677–688.

Pethig, R. 1996. Dielectrophoresis: using inhomogeneous AC electrical fields to separate and manipulate cells. *Crit. Rev. Biotechnol.* 16: 331–348.

Pethig, R., Y. Huang, X. B. Wang, and J. Burt. 1992. Positive and negative dielectrophoretic collection of colloidal particles using interdigitated castellated microelectrodes. *J. Phys. D.-Appl. Phys.* 25:881–888.

Pohl, H. A. 1978. Dielectrophoresis: The Behavior of Neutral Matter in Nonuniform Electric Fields. Cambridge University Press, Cambridge, UK.

Porschke, D. 1985. The mechanism of ion polarization along DNA double helices. *Biophys. Chem.* 22:237–247.

Ren, K. F., G. Grehan, and G. Gouesbet. 1996. Prediction of reverse radiation pressure by generalized Lorenz-Mie theory. *Appl. Opt.* 35: 2702–2710.

Rousselet, J., L. Salome, L. Adjari, and J. Prost. 1994. Directional motion of Brownian particles induced by a periodic asymmetric potential. *Nature.* 370:446–448.

Smith, S. B., L. Finzi, and C. Bustamante. 1992. Direct mechanical measurements of the elasticity of single DNA molecules by using magnetic beads. *Science.* 258:1122–1126.

Smith, S. B., C. Yujia, and C. Bustamante. 1996. Overstretching B-DNA: the elastic response of individual double-stranded and single-stranded DNA molecules. *Science.* 271:795–799.

Takashima, S. 1963. Dielectric dispersion of DNA. *J. Mol. Biol.* 7:455–467.

Takashima, S. 1989. Electrical Properties of Biopolymers and Membranes. IOP, Philadelphia, PA.

Tinland, B., A. Pluen, J. Sturm, and G. Weill. 1997. Persistence length of single-stranded DNA. *Macromolecules.* 30:5763–5765.

Volkmuth, W. D., T. Duke, M. C. Wu, R. H. Austin, and A. Szabo. 1994. DNA electrodiffusion in a 2-D array of posts. *Phys. Rev. Lett.* 72: 2117–2120.

Washizu, M., and O. Kurosawa. 1990. Electrostatic manipulation of DNA in microfabricated structures. *IEEE Trans. Ind. Appl.* 26:1165–1172.

Washizu, M., S. Suzuki, O. Kurosawa, T. Nishizaka, and T. Shinohara. 1994. Molecular dielectrophoresis of biopolymers. *IEEE Trans. Ind. Appl.* 30:835–843.

Yang, J., Y. Huang, X. B. Wang, F. F. Becker, and P. Gascoyne. 1999. Cell separation on microfabricated electrodes using dielectrophoretic/gravitational field flow fractionation. *Anal. Chem.* 71:911–918.